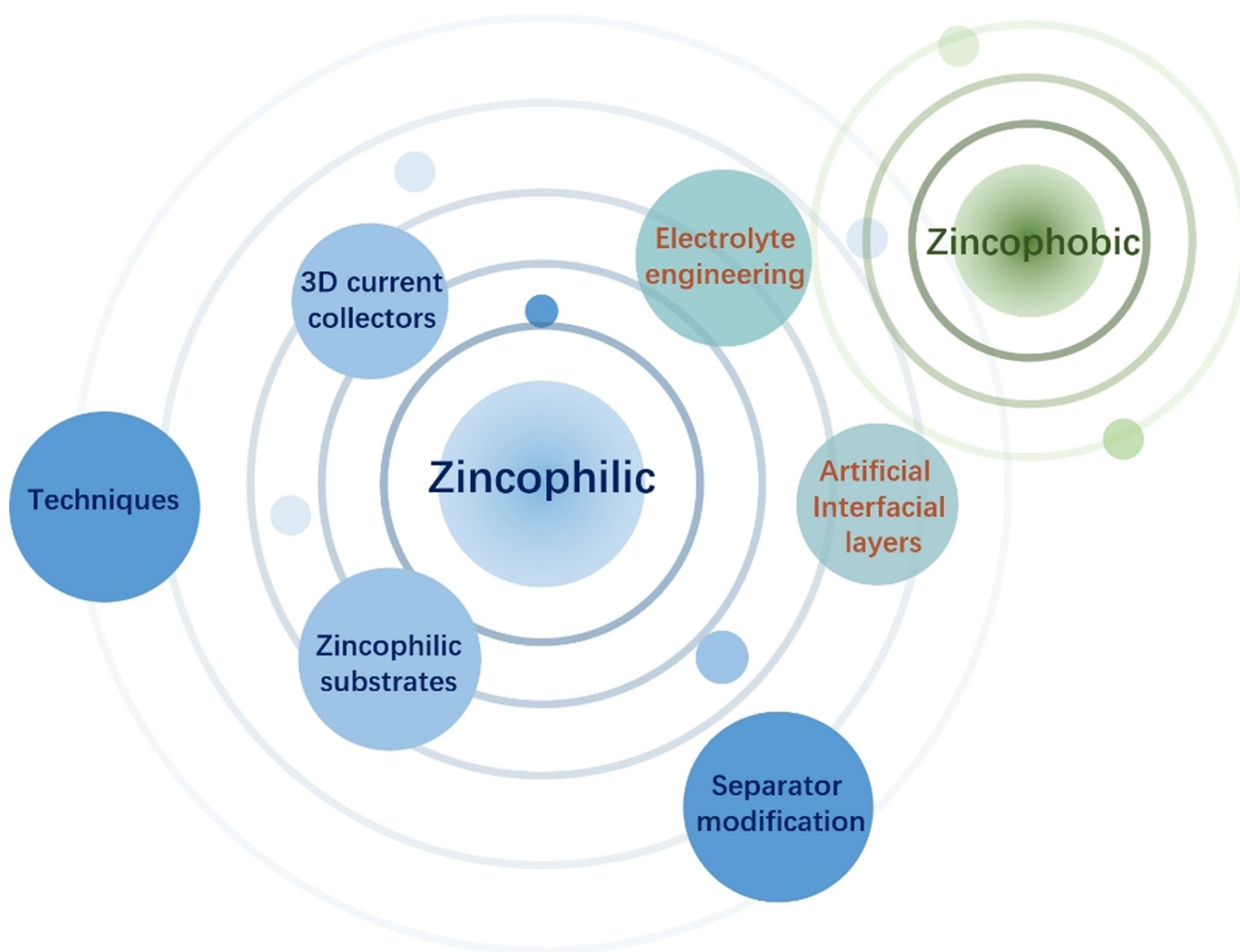


# Zincophilic Design and the Electrode/Electrolyte Interface for Aqueous Zinc-Ion Batteries: A Review

Chenyang Zhao,<sup>[a]</sup> Yu Zhang,<sup>[b]</sup> Jiaze Gao,<sup>[c]</sup> Zhikun Guo,<sup>[a]</sup> Aosai Chen,<sup>[a]</sup> Nannan Liu,<sup>[a]</sup> Xingyuan Lu,<sup>[a]</sup> Xigui Zhang,<sup>\*[d]</sup> and Naiqing Zhang<sup>\*[a]</sup>



Aqueous zinc-ion batteries (ZIBs) are limited in energy storage by the persistent Zn dendrites, which is a major bottleneck preventing the commercial application of rechargeable aqueous zinc-ion batteries. The dendritic problems associated with Zn metal anodes can lead to rapid performance degradation, failure and even safety risks of the battery. Zincophilicity of the electrode/electrolyte interface is critical to the stable and safe operation for aqueous ZIBs. In this review, we discuss that zincophilicity can be regulated by tuning the chemical inter-

actions of material surface energy with zinc metal, emphasizing the importance of zincophilic design for improving the electrochemical performance of zinc electrodes. Advances in optimization strategies for the zincophilic zinc metal anode/electrolyte interface are summarized. Challenges and prospects for further exploration and balance of zincophilicity of the anode/electrolyte interface are presented, which are expected to promote in-depth research and practical applications of advanced aqueous zinc ions.

## 1. Introduction

In recent years, lithium-ion batteries (LIBs) have become an advanced energy storage system attracting attention.<sup>[1]</sup> However, the increasing cost and safety problems of LIBs have forced researchers to explore energy storage systems with high safety, environmental friendliness and low cost. The aqueous zinc-ion battery (ZIBs) stands out because of its advantages of using highly safe waterborne electrolyte. At the same time, the metal zinc as the waterborne zinc ion anode has low cost, non-toxic, abundant reserves, low redox potential ( $-0.76$  V relative to standard hydrogen electrodes) and high theoretical volume capacity ( $5851 \text{ mAh cm}^{-3}$ ).<sup>[2,3]</sup> In view of such advantages, ZIB are assembled in air, which can greatly reduce the cost while ensuring the safety, and enhance the potential of future commercial applications. However, the service life of ZIB is seriously limited by the problem of Zn dendrite.<sup>[4]</sup> Due to the non-uniform transport of Zn ions during the continuous plating/stripping process, many non-uniform Zn crystals are often produced during the initial nucleation stage. Subsequently, these zinc crystals will continue to grow and eventually become deadly zinc dendrites.<sup>[5]</sup> The sharp needle shaped zinc dendrites increase the risk of penetrating the diaphragm, which will lead to internal short circuit and failure of the battery. These problems lead to limited cycle life and dendrite problems related to zinc metal anode, which may lead to rapid decline in battery performance, failure and even safety risks. Zincophilicity of the anode/electrolyte interface is critical to the stable and safe operation of aqueous zinc-ion batteries.

Zincophilicity is a definition derived from lithophilicity,<sup>[6]</sup> the affinity of an interface for zinc, which measures the difficulty of zinc deposition on the substrate and guides the initial nucleation and subsequent growth of zinc. The concept of zincophilicity was first applied to the protection design of zinc anodes by Pan et al. in 2019.<sup>[7]</sup>

Zincophilicity can be regulated by adjusting the material surface energy and chemical interactions with zinc metal. The surface energy or binding energy has a significant influence on the zincophilicity of the electrolyte and is highly dependent on the chemical composition of the SEI. In addition to this, the zincophilicity can be modulated by introducing additional chemical interactions at the interface. For example, the selection of a metallic substrate capable of metal-zinc-generating alloys can effectively show some improvement of the interfacial contact between the zinc anode and the solid electrolyte. Zincophilicity is characterized by the nucleation barrier in electrochemical tests, and high zincophilicity reduces the Zn nucleation barrier and form a stable structure with the zinc. Thus, Zn nucleation and subsequent uniform deposition began to take shape. Notably, according to the Wenzel model, adjusting the surface roughness is an effective method for regulating the lithophilicity of liquid lithium. In contrast, unlike lithium, metallic Zn cannot be judged by the direct contact of molten state Zn with the material because of its high melting point, so there are no studies to adjust the surface roughness of the material to prove its zincophilicity.<sup>[8]</sup> This review aims to enrich the current understanding of zincophilicity at the zinc metal anode/electrolyte interface of aqueous zinc ion batteries and its impact on the battery performance, emphasizing the importance of zincophilic design for polishing up the electrochemical performance of ZIBs. For the zincophilic zinc metal anode/electrolyte interface, strategies such as improving the zincophilic substrate, constructing in situ/ex situ artificial interfacial layers, optimizing the 3D current collector, and modifying the diaphragm are summarized, in addition, we also discuss the mechanism of zincophobicity and integrated zincophilic/zincophobic modulation and the improvement of zinc metal anode performance (Figure 1). We conclude by looking at the prospects and challenges of zincophilic design so that we can address the interfacial challenges and provide insights and strategies to improve battery performance.

- [a] C. Zhao, Z. Guo, A. Chen, N. Liu, X. Lu, Prof. N. Zhang  
State Key Laboratory of Urban Water Resource and Environment  
School of Chemistry and Chemical Engineering  
Institution Harbin Institute of Technology  
92 Xidazhi Street, Nangang District, Harbin, 150001 (China)  
E-mail: znmww@163.com
- [b] Dr. Y. Zhang  
School of Energy Science and Engineering  
Institution Harbin Institute of Technology  
92 Xidazhi Street, Nangang District, Harbin, 150001 (China)
- [c] J. Gao  
Shen Zhen College of International Education  
3 Antuoshan 6th Rd Futian (China)
- [d] Prof. X. Zhang  
Dleta Institute (Huzhou), University of Electronic Science and Technology of China, Huzhou, 313001 (China)  
E-mail: zxgfc2008@hotmail.com

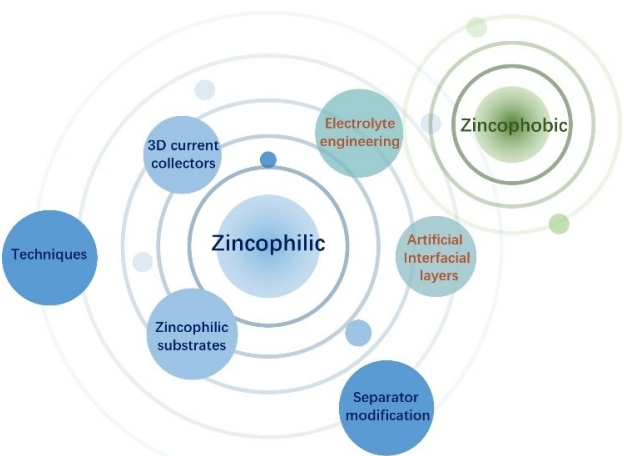


**Figure 1.** Schematic diagram of the solution strategies to modulate the zincophilicity/zincophobie of the interface of electrode/electrolyte, such as zincophilic substrates, artificial interfacial layers, three-dimensional (3D) current collectors, electrolyte engineering, separator modification, techniques, zincophobie design and zincophilicity-zincophobie combination design.

## 2. Zincophilic Substrates

### 2.1. Alloy based substrates

Lu et al.<sup>[9]</sup> electrochemically deposited zinc on the surface of the alloy Cu–Zn (CZ–Zn), and revealed that the zincophilic Cu sites of CZ–Zn can significantly increase the adsorption of Zn<sup>2+</sup> and assist the uniform initial nucleation of Zn, producing a

dendrite-free Zn anode (Figure 2a). Lou et al.<sup>[10]</sup> designed and developed a three-dimensional multifunctional host (Cu NBs@NCFs) composed of N-doped carbon fibers implanted in Cu nano boxes. The zincophilic Cu and the Cu–Zn alloy formed in situ can be used as homogeneous nucleation sites to reduce the overpotential of nucleation of Zn and guide the deposition of homogeneous and dense Zn. Lee et al.<sup>[11]</sup> activated a Cu–Zn alloying reaction through a deep eutectic solvent to manufacture an interlayer of zincophilic Zn-rich alloy. The alloy layer forms dense zinc coating after zinc deposition that could tolerate continuous cycling in aqueous electrolytes and effectively prevent ZIBs corrosion and swelling. Jiang et al.<sup>[12]</sup> demonstrated that in situ surface alloying of Cu and Zn assisted by anionic surfactants significantly improved the invertibility of Zn in 3D nanoporous Zn<sub>x</sub>Cu<sub>y</sub>/Zn electrode. Because of its zero nucleation overvoltage, the zincophilic Zn<sub>x</sub>Cu<sub>y</sub> alloy can guide the uniform deposition of zinc, and promote the stripping process of zinc through the electrical coupling of Zn<sub>x</sub>Cu<sub>y</sub>/Zn. Moreover, the self-supported nanoporous Zn<sub>x</sub>Cu<sub>y</sub>/Zn electrode exhibited excellent stripping/plating behavior in aqueous electrolyte without dendrite, excellent cycle stability and high zinc utilization rate after 1900 hours.

Except for Cu, Sb,<sup>[13,14]</sup> Sn<sup>[15]</sup> and Bi<sup>[16]</sup> are also shown high zincophilic properties. Xue et al.<sup>[13]</sup> designed an in situ homogeneous and robust protective layer of metallic antimony on the zinc anode surface by substitution reaction. The Zn@Sb anode provides vivid zincophilic sites to guide even Zn nucleation and uniform electric field on the surface of the Zn anode, both of which favor forming uniform Zn deposition. Feng et al.<sup>[14]</sup> designed multifunctional homogeneous antimony (Sb) nano-

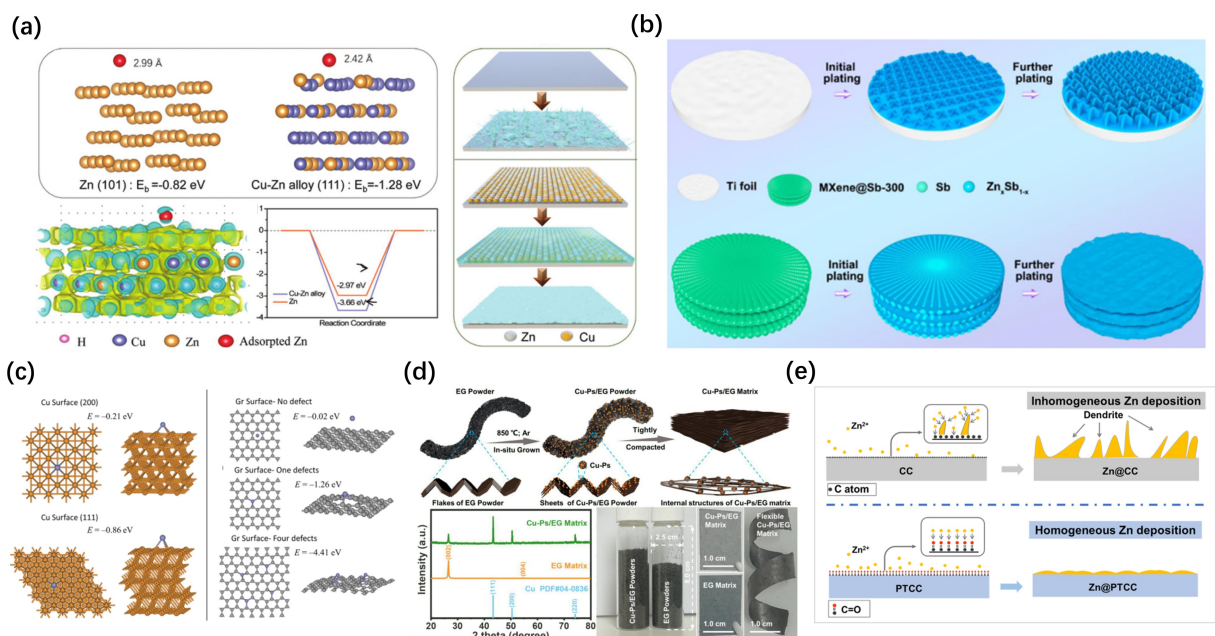


**Figure 2.** a) DFT calculation of Zn (101) and Cu–Zn alloy (111), and the schematic representing Zn deposition behavior on the Zn and CZ–Zn anodes before and after cycles. Produced with permission from Ref. [9]. Copyright (2021) Wiley-VCH. b) The schematic diagrams for MXene@Sb-300 and Ti foil during plating. Produced with permission from Ref. [14]. Copyright (2021) Elsevier B.V. c) Zn atom adsorption structures and the corresponding binding energies of Cu (200), Cu (111), pristine Gr, Gr with single defect and Gr with four defects. Produced with permission from Ref. [17]. Copyright (2019) American Chemical Society. d) Schematic illustration of Cu–Ps/EG matrix. Adapted with permission from Ref. [18]. Copyright (2022) Elsevier B.V. e) The schematic diagrams of zinc deposition evolution on CC and PTCC electrodes. Produced with permission from Ref. [19]. Copyright (2022) The Author(s). Published by Frontiers Media Sa.

arrays and grew them on  $Ti_3C_2T_x$  MXene paper (Figure 2b). It was discovered that antimony could be reversibly alloyed with Zn to form ZnSb, which allows antimony to act as both an alloyed Zn storage material and as a zincophilic nucleation seed to regulate a dendrite-free morphology.

## 2.2. Carbon based substrates

Reza et al.<sup>[17]</sup> provided a low nucleation overpotential point for the deposition of Zn through demonstrating monolayer graphene (Gr) as an electrodeposition carbon based substrate due to the high lattice compatibility of the Gr layer with the Zn, which is shown in Figure 2(c). DFT calculations showed that Gr has high zincophilicity due to the binding energy of Gr with four defect sites is 4.41 eV for Zn, leading to the low interfacial energy between Gr and Zn ( $0.212\text{ J m}^{-2}$ ). This synergistic compatibility promotes the subsequent uniform and planar Zn deposition, which achieves a compact and homogeneous structure, thus greatly enhancing the electrochemical stability of the ZIBs.

## 2.3. Alloy & carbon composite substrates

Hou et al.<sup>[18]</sup> reported a flexible zinc anode (Zn@Cu–Ps/ EG) in situ prepared by expanded graphite (EG) modified by copper particles (Cu–Ps) without dendrite in Figure 2(d). On the one hand, Cu can form intense interactions with carbon during the heating process, stabilizing the structure of the complex substrates, increasing the cycle performance of Zn anode, and on the other hand, Cu as a zincophilic seed, can reduce the nucleation overpotential of Zn. In situ construction of zincophilic Cu on EG substrate is conducive to lower the electrodeposition overpotential and improving the mechanical strength of zinc-ion battery, thus enhancing the cycle stability of ZIBs. Kang et al.<sup>[19]</sup> used a simple oxygen plasma treatment to change the surface state of carbon cloth to build a dendrite-free substrate for Zn plating and to solve the problem of dendrites of Zn anodes (Figure 2e). The zincophilic C=O nucleation sites uniformly distributed on the plasma treated carbon cloth (PTCC) electrode make the electrode have low nucleation overpotential, which is conducive to the initial homogeneous nucleation of zinc and subsequent deposition.

The alloy substrates have high conductivity and structural stability, and provides a large number of zincophilic sites, which is conducive to the subsequent deposition of zinc. Carbon substrates usually have high conductivity, high specific surface area and rich pore structure, which can uniform zinc ion flux, promote the diffusion of zinc ion and provide more load space for zinc deposition. The combination of the above can increase the zincophilic sites of the substrate while maintaining a rich load space, which is conducive to the deposition of zinc in universities. However, the initially deposited zinc will completely cover the zincophilic sites, resulting in the subsequent deposition of zinc growing on the initially deposited zinc instead of the zincophilic sites provided by the substrate. To

some extent deviates from the original intention of constructing the zincophilic sites to guide the uniform deposition of zinc, which still needs further consideration and solutions from researchers.

## 3. Artificial Interfacial Layers

The morphology of zinc deposition at the anode is closely related to the spread of  $Zn^{2+}$  at the interface of electrode and electrolyte. However, the passivation layer on the surface of Zn anode in neutral or weakly acidic aqueous electrolytes is usually inhomogeneous and unstable. In addition, the anions in commonly used  $ZnSO_4$  or  $Zn(CF_3SO_3)_2$  electrolytes are electrochemically stable in the electrolyte and not able to form a zinc ion conductive solid electrolyte interface on the zinc cathode surface, which leads to uneven distribution of zinc ion flux on the electrode surface, which leads to dendritic growth in the process of plating/stripping.

On account of the successful experience with artificial interfacial layers for lithium metal anodes, the construction of effective artificial interfacial layers on Zn anodes to adjust Zn ion flux and guide uniform Zn deposition is a promising strategy.<sup>[20,21]</sup> In the current research, there are two main strategies for building artificial interfacial layers, including by direct surface coating<sup>[22]</sup> as well as chemical/electrochemical reactions on the zinc metal surface.<sup>[23]</sup>

### 3.1. Ex situ artificial interfacial layers

#### 3.1.1. Inorganic interfacial layer

Chen et al.<sup>[24]</sup> fabricated a fluorine-doped amorphous carbon (CF) interfacial layer on top of the Cu collector (CF–Cu) by simply carbonizing of the fluoropolymer coating for the underlying Zn deposition (Figure 3a, b). The fluorine atom, as an abundant zincophilic site, regulates the rapid transfer kinetics of Zn ions, which was partially converted into  $ZnF_2$  as a  $Zn^{2+}$  conductor to regulate the homogeneous deposition of Zn.

Artificial interfacial films of nitrogen (N)-doped graphene oxide (NGO) were designed by Chen et al.<sup>[25]</sup> using the Langmuir–Blodgett method to form parallel and ultrathin interfacially modified layers on Zn foils. The directional deposition of Zn crystals in the (002) plane was announced due to the favorable zincophilic properties of the parallel graphene layers and N-doped groups. Young et al.<sup>[26]</sup> constructed layered nanostructured layers by mesoporous zincophilic  $TiO_2$  nanoparticles and chemically adapted to Zn dendrite formation. This layered zincophilic  $TiO_2$  layer on the anode surface is crucial to restrain zinc dendrites and improving the electrochemical performance of the ZIBs. Lee et al.<sup>[27]</sup> constructed robust zincophilicity channels on Zn anodes based on carboxylated hollow cerium dioxide nanostructures. With the robust 3D nanostructures, at current densities of  $3\text{ mA cm}^{-2}$  for nearly 2000 h, the zincophilic channel interfaces on zinc anodes exhibited highly plating/stripping cycle stability. Feng et al.<sup>[28]</sup>

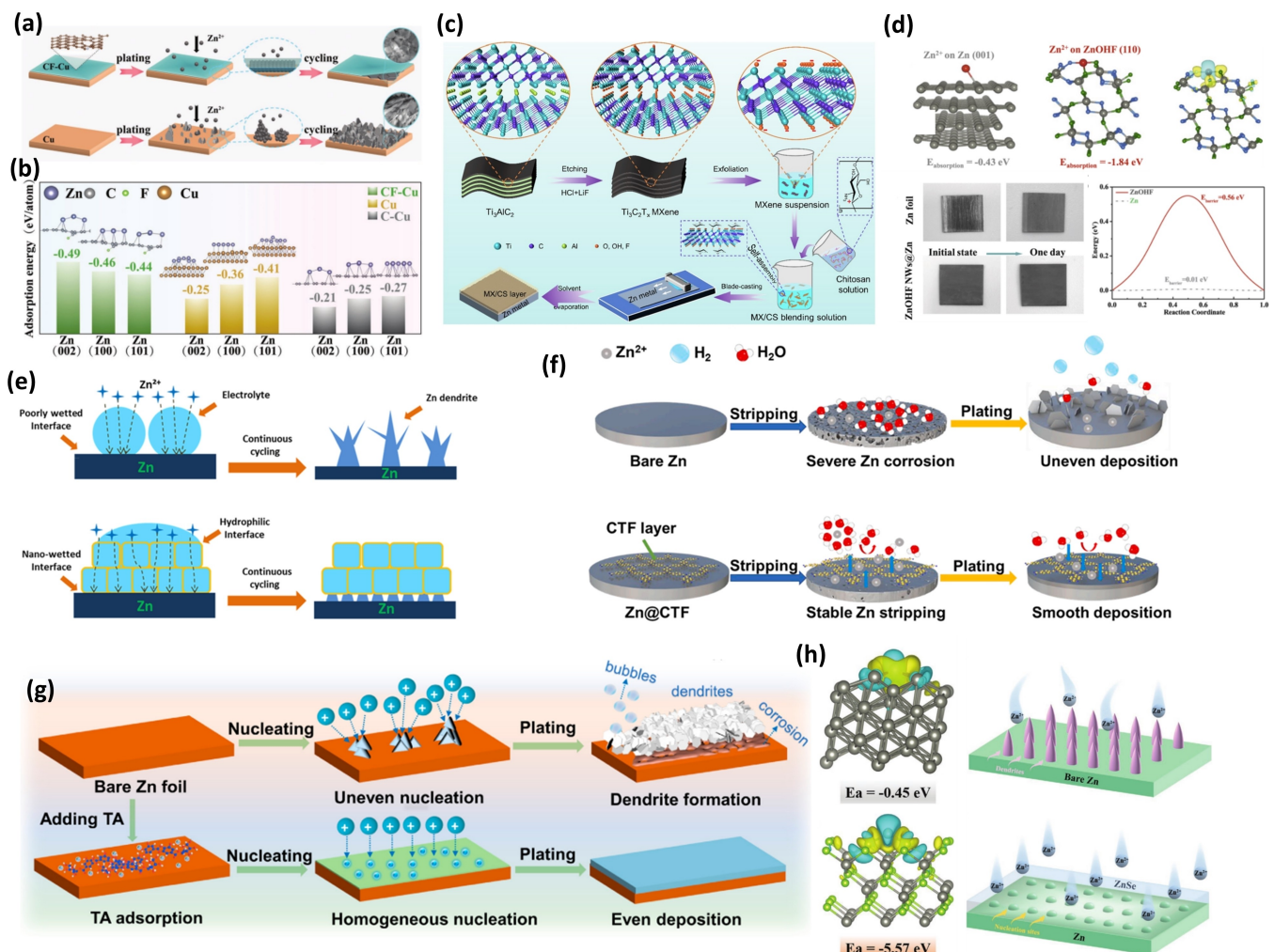


**Figure 3.** a) The schematic diagrams of Zn deposition on CF-Cu and Cu. b) Adsorption energy of  $\text{Zn}(002)$ ,  $\text{Zn}(100)$ ,  $\text{Zn}(101)$  on CF, C and Cu(111). Produced with permission from Ref. [24]. Copyright (2022) Wiley-VCH. c) Schematic presentation of fabricating MX/CS-Zn anode. Adapted with permission from Ref. [28]. Copyright (2021) Elsevier B.V. d) The calculated binding energy, photographs and activation energy for migration of  $\text{Zn}^{2+}$  on Zn (001) and ZnOHF (110). Adapted with permission from Ref. [30]. Copyright (2022) Elsevier B.V. e) The plating process of Zn on Bare Zn and MOF-PVDF-Coated Zn. Produced with permission from Ref. [7]. Copyright (2019) American Chemical Society. f) The stripping and plating diagrams of Zn deposition on bare Zn and Zn@CTF electrodes. Adapted with permission from Ref. [31]. Copyright (2022) Elsevier B.V. g) The Zn deposition process of bare Zn and TA@Zn. Produced with permission from Ref. [32]. Copyright (2022) The Author(s). Published by Frontiers Media Sa. h) Charge density differences and schematic illustration of Zn deposition mechanism on Zn and ZnSe@Zn. Produced with permission from Ref. [33]. Copyright (2021) Wiley-VCH.

designed a flexible MXene film to adhere to the surface of zinc as an artificial interface (Figure 3c). This amine-rich protective film not only effectively prevents zinc from water corrosion, but also promotes zinc nucleation and subsequent uniform plating/stripping due to the strong coordination between  $\text{Zn}^{2+}$  and amino group. Ye et al.<sup>[29]</sup> constructed in situ tetramethylammonium intercalated  $\text{Ti}_3\text{C}_2\text{T}_x$  MXene (MX-TMA) coatings with low zinc nucleation barriers on zinc foil surfaces. It provided IPL with abundant zincophilic sites and better hydrophilicity, promoted  $\text{Zn}^{2+}$  transport for uniform electrodeposition, and suppressed interfacial side reactions. In addition, the deposition of Zn on the beneficial (002) planes was further revealed under the guidance of MX-TMA.

Wang et al.<sup>[30]</sup> constructed three-dimensional ZnOHF nanowire array interfaces (ZnOHF NWs@Zn) in situ on Zn foil. As a  $\text{Zn}^{2+}$  ion modulation layers, ZnOHF guides the long-period of

zinc plating/stripping process. Compared with bare zinc, ZnOHF shows superior zincophilicity, resulting in lower zinc nucleation barrier and uniform zinc deposition. As shown in Figure 3(d), in terms of adsorption energy, the value of  $\text{Zn}^{2+}$  ions adsorbed on ZnOHF (110) surface is apparently higher than that of Zn, indicating a better zincophilicity of ZnOHF compared to the bare Zn. Due to the strong interaction between  $\text{Zn}^{2+}$  and ZnOHF, interface charge distribution gets balance, which precipitates the diffusion of  $\text{Zn}^{2+}$  and prevents a large number of zinc ions from gathering on bare Zn to form zinc dendrites, which guides the uniform plating of Zn on ZnOHF.

Zhang et al.<sup>[34]</sup> used a freestanding hydroxylated carbon nanotube (OH-CNT) film as an artificial interfacial layer of Zn anode. Hydroxyl group, as the zincophilic functional group of carbon nanotubes, provides a large number of zinc loving sites, and homogenizes the subsequent deposition of zinc. CNT

membranes also allow for uniform distribution of Zn ion and electron for uniform growth of zinc. Consequently, symmetric cells exhibit a low overpotential of 83 mV and excellent performance during plating and stripping procedures over 500 h without dendrites. A thin, mesoporous polypyrrole (PPy) paper was proposed by Wang and co-workers<sup>[35]</sup> as a zincophilicity coating, and the high surface area of the PPy coating contributed to increased kinetics of the reaction and uniform pore size distribution for uniform  $Zn^{2+}$  flux. Thus, the modulation of the PPy coating with engineered surface flatness resulted in excellent cycling performance of Zn anode over 930 h at a high current density of  $5 \text{ mAh cm}^{-2}$ . Two-dimensional conductive graphite (KS-6) layer was proposed with a high electronic conductivity (similar to  $10^6 \text{ S m}^{-1}$ ) by Wang et al.,<sup>[36]</sup> which form a strong bond directly to the Zn metal due to their high zincophilicity, thus protecting the Zn anode from the electrolyte to inhibit hydrogen evolution side reaction and to direct zinc deposition without dendrites.

### 3.1.2. Organic interfacial layer

Here, composites composed of reactions between organic monomers and linkers such as MOFs and COFs are also classified in the organic interfacial layer. Pan et al.<sup>[7]</sup> designed a composite coating made up of nano-metal organic frameworks (MOFs) to enhance the detrimental wetting effect of aqueous electrolytes on zinc metal and reconstruct the interface of anode/electrolyte in Figure 3(e). A nanoscale wetting effect was achieved, and electrolyte flux was regulated through the hydrophilic MOF nanoparticle. Significant charge transfer resistance was observed at the constructed zincophilic interface. As a result, modified anode exhibited high electrochemistry performance for more than 500 cycles. Long et al.<sup>[37]</sup> made a multifunctional interface layer based on zeolitic imidazole framework (ZIF-11). The interface layer contains zincophilic nitrogen-containing functional groups, which form a thin double electric layer by strongly adsorbing zinc ions on the channel wall in the interface layer. The double electric layer leads to flat the electric conduction of surface and stable deionization impact in the channel, cooperatively guiding uniform zinc ion flux, so that uniformly deposition can be got. Li et al.<sup>[38]</sup> in situ grow ZnO on ZIF-8 to synthesize ZnO@ZIF-8 modified layer. The ordered nanochannels and abundant abundant nitrogen species of ZnO@ZIF-8 provide zincophilic sites for Zn deposition and construct dendrite-free Zn anodes. A negatively charged metal organic framework (UIO-66-SO<sub>3</sub>H) layer was designed on Zn anode by Wang et al.<sup>[39]</sup> The interfacial layer with zincophilic SO<sub>3</sub> functional groups unifies the flux of  $Zn^{2+}$  flux and uniform the deposition of Zn, and inhibits dendritic crystals and side reactions.

Lan et al.<sup>[40]</sup> designed COFs (i.e., Zn-AAm-COF, Zn-DAAQ-COF, Zn-DAA-COF) with structures rationally selected to have structural pillars with polar groups or zincophilic groups that provide a high degree of interaction with  $Zn^{2+}$ , water molecules, and zinc surfaces, thus promoting the generation of zincophilic layers, electrolyte/electrode wetting and  $Zn^{2+}$

jumping/deposition. To address these issues, Li et al.<sup>[31]</sup> prepared covalent triazine frameworks (CTFs) with rich zinc ion transfer channels and strong chemical stability as zinc anode coatings. Triazine ring with abundant nitrogen species has strongly zincophilic, increasing the kinetics of zinc deposition and promoting the homogeneous nucleation of Zn (Figure 3f). Zhao et al.<sup>[41]</sup> fabricated zincophilic covalent organic framework films by interfacial reactions (TpPa-SO<sub>3</sub>H@Zn-foil). The covalently bound and off-domain sulfonates lead to a low nucleation overpotential and uniformly zinc deposition. Meanwhile, the sulfonate group of TpPa-SO<sub>3</sub>H film can attached to the  $Zn^{2+}$  to decrease the solvation potential of Zn, forming abundant Zn transport channels and inhibiting the diffusion of two-dimensional Zn ions.

Yang et al.<sup>[42]</sup> prepared a nanoarray structure consisting of zincophilic MOF sheets as the zinc anode modification layer. The sites of zinophilic N and O can realize the uniform pre deposition of zinc ions, and then zinc is horizontally deposited on these sheets from bottom to top, finally forming a U-shaped deposition along the nano array. Therefore, the 2D zinophilic MOF composite zinc anode has achieved significantly enhanced the reversible process of plating/stripping. Under the current density of  $5 \text{ mA cm}^{-2}$  and the low over-voltage of 50 mV, it has a long durability of 1880 hours. A polyanionic hydrogel film was introduced by Fan et al.<sup>[43]</sup> as an artificial layer for zinc anodes with the aid of a silane coupling agent (denoted as Zn-SHn). The SO<sub>3</sub> functional groups make the flux and transport of zinc ions on the hydrogel framework more uniform.

### 3.2. In situ artificial interfacial layers

Kang et al.<sup>[44]</sup> proposed a general and multifunctional complex metal-organic phase strategy to achieve rapid and homogeneous zinc deposition for long-period zinc ion batteries. In situ complexing the metal-phytate interphase constructed a zincophilic interface that uniform the nucleation and further deposition of Zn in terms of kinetics. He et al.<sup>[32]</sup> soaked metallic Zn into tannic acid (TA) solution and constructed a metal chelate anode (TA@Zn) with high zincophilicity on the metallic Zn surface (Figure 3g). Taking advantage of the generous hydrophilic and zincophilic phenolic hydroxyl groups of TA, the  $Zn^{2+}$  are strongly attracted to the metal chelate interlayers, guiding the uniform deposition of zinc and reducing the  $Zn^{2+}$  migration barriers. Yang et al.<sup>[33]</sup> proposed a modified zinc foil with a zincophilic ZnSe layer deposited though the selenization process. The stronger adsorption capacity for  $Zn^{2+}$  ions and the order of magnitude of homogeneous ion diffusion channels of ZnSe lead to lower barriers to formation and faster ion diffusion kinetics (Figure 3h). At the same time, the harmful zinc corrosion in the aqueous system is effectively mitigated.

Jiang et al.<sup>[45]</sup> constructed a HML layer with high conductivity and high zincophilicity for a uniform zinc anode by in-situ forming a heterogeneous metal layer (HML) on the surface of zinc metal, which can further reduce the nucleation barrier and inhibit dendrite formation. In addition, HML has a large number of micropores and large specific surface area, which further

alleviates the volume expansion during the process of plating/stripping, ensuring the rapid transfer of  $Zn^{2+}$ , regulating the uniform deposition of  $Zn^{2+}$ , and enhancing the cycle life of ZIBs.

Although the effective artificial interface layers were constructed on the zinc anode to regulate the zinc ion flux and guide the uniform deposition of zinc, improving the electrochemical performance of the zinc anode. It is difficult to regulate the zinc deposition behavior in an ideal and stable way during the long cycle and high rate plating and stripping process. During the long-term cycle of high current density or low current density, the volume of zinc anode will change dramatically. The inelastic artificial interface layer is probably to produce cracks, damage its integrity, reduce the protection function, and the zincophilic sites are no longer uniformly distributed. It is necessary to further improve the construction of the interface layer to enhance its protection effect.

#### 4. Three-dimensional (3D) current collectors

The 3D structure provides an enormous internal space to accommodate the deposition of Zn, reducing the local current density, alleviating the tip effect to inhibit the zinc dendrites and lightening the volume expansion of zinc metal anode. By improving the zincophilicity between the current collector surface and electrolyte, an adaptive negative body with uniform nucleation is achieved, uniformity of current distribution and volume variation, which becomes an effective means to alleviate the dendrite problem.

##### 4.1. 3D carbon current collectors

You et al.<sup>[46]</sup> reported an efficient method to control the viscosity of the liquid crystal SWCNT phase for fiber spinning. By functionalizing single-walled carbon nanotubes with tris(hydroxymethyl)aminomethane (THA), it was shown that as well-distributed zincophilic sites. Yao et al.<sup>[47]</sup> used highly conductive 3D carbon fiber skeletons (ZnO and CFs) precoated with super-hydrophilic ZnO on the surface of zinc anodes (Figure 4a). It is expected that ZnO induces the Zn nucleation and retards dendrite generation and CFs skeletons reduce the local current density to uniform the Zn ion flow and to relieve the overall stress during Zn plating and stripping. Li et al.<sup>[48]</sup> proposed that a three-dimensional porous hollow fiber framework with  $TiO_2$ ,  $SiO_2$  and carbon as a hydrophilic current collector for Zn anodes. Even at ultra-high current densities, the amorphous  $TiO_2$  and  $SiO_2$  zinc to nucleate and deposit in porous hollow fibers. Chen et al.<sup>[43]</sup> prepared a 3D porous graphene carbon nanotube scaffold modified with MOF derived ZnO/C nanoparticles as a collector of zinc anodes. ZnO nanoparticles have highly zincophilicity and play the role of seed for zinc pre nucleation. Due to the low nucleation potential barrier of ZnO, the zinc can uniform deposition on the anode. Lu<sup>[49]</sup> designed carbon fiber (ZFCF) rich in N, O functional groups as the host of zinc anode. Based on the DFT

calculation, it is confirmed that due to the stronger adsorption of Zn on the zincophilic functional sites on the N and O surfaces and the porous structure between carbon fiber (CF) bundles, the growth of Zn dendrites is inhibited, and zinc can grow uniformly on the anode.

The gelation process was directed by Chen et al.<sup>[50]</sup> for the creation of flexible MXene/graphene scaffolds. In the electroplating process, zinc is tightly wrapped in the rich micropores of the host. In the cycle process, because MXene contains fluorine atoms, the composite anode generates zincophilic zinc fluoride from fluorine atoms in MXene at the electrode/electrolyte interface, which induces the uniform deposition of zinc, thus effectively inhibiting the generation of zinc dendrites. Furthermore, foldable 3D MXene and graphene aerogel composite materials have been shown to be highly zincophilic skeletons appealed by structural changes. By one-step electrodeposition, the heterogeneous body firmly distributes the bulk Zn in a 3D microscale manner.

Lou et al.<sup>[51]</sup> developed a  $TiO_x/Zn/N$ -doped carbon antipodal opal substrate to regulate Zn deposition. In order to reduce the nucleation overpotential and avoid the precipitation of hydrogen, amorphous  $TiO_x$  and N-doped carbon were utilized as zincophilic sites. Fan et al.<sup>[52]</sup> designed a unique 3D microscaffold (Sn-PCF) shown in Figure 4(b). Zincophilic Sn nanodots are coupled in 3D cross-linked carbon fiber arrays to build a host for dendrite-free zinc anode. The "tip effect" is effectively eliminated by uniforming the current density by building restraints for the dendrites. Metallic Sn shows strong  $Zn^{2+}$  adsorption and fast  $Zn^{2+}$  surface diffusion on the surface of Zn, which are key to regulating nucleation and uniform Zn deposition.

Shao et al.<sup>[57]</sup> designed ultrathin  $NH_4V_4O_{10}$  film-modified carbon fabric to achieve a zinc metal anode without dendrite, which may serve as a site for zinc nucleation to effectively reduce the overpotential for uniform deposition of zinc. Wang et al.<sup>[58]</sup> designed highly zincophilic 3D MOF-derived carbon with nitrogen and oxygen functional groups (N,O-MOFC) scaffolds on the basis of theoretical calculations guided by electrodeposition chemistry by adjusting the initial nucleation and further growth of the zinc metal. By adjusting the electrodeposition chemistry on layered 3D nanostructures, high-performance 3D zincophilic anodes (Zn/N, O-MOFC-CNTF) with adjustable deposition morphology are realized, which enhance the adsorption energy of zinc, reduce the deposition overpotential of zinc, and achieve high energy density and long-term stability of zinc ion batteries.

Wang et al.<sup>[59]</sup> synthesized oxygen and nitrogen co-doped carbon superstructures as effective carriers for high electrical charging depth of zinc metal anodes through reasonable structural design. Density flooding theory (DFT) calculations showed that the ether (C–O), the carboxylic acid and pyrrolidine N groups exhibited strong binding to Zn in the oxygen/nitrogen dopant, which made the favorable sites 4 heterogeneous nucleation for the growth of zinc. Therefore, the monomers rich in these O/N groups are reasonably selected and converted into carbon with different shapes and sizes, and abundant mesopores/macropores dopants to prepare corre-

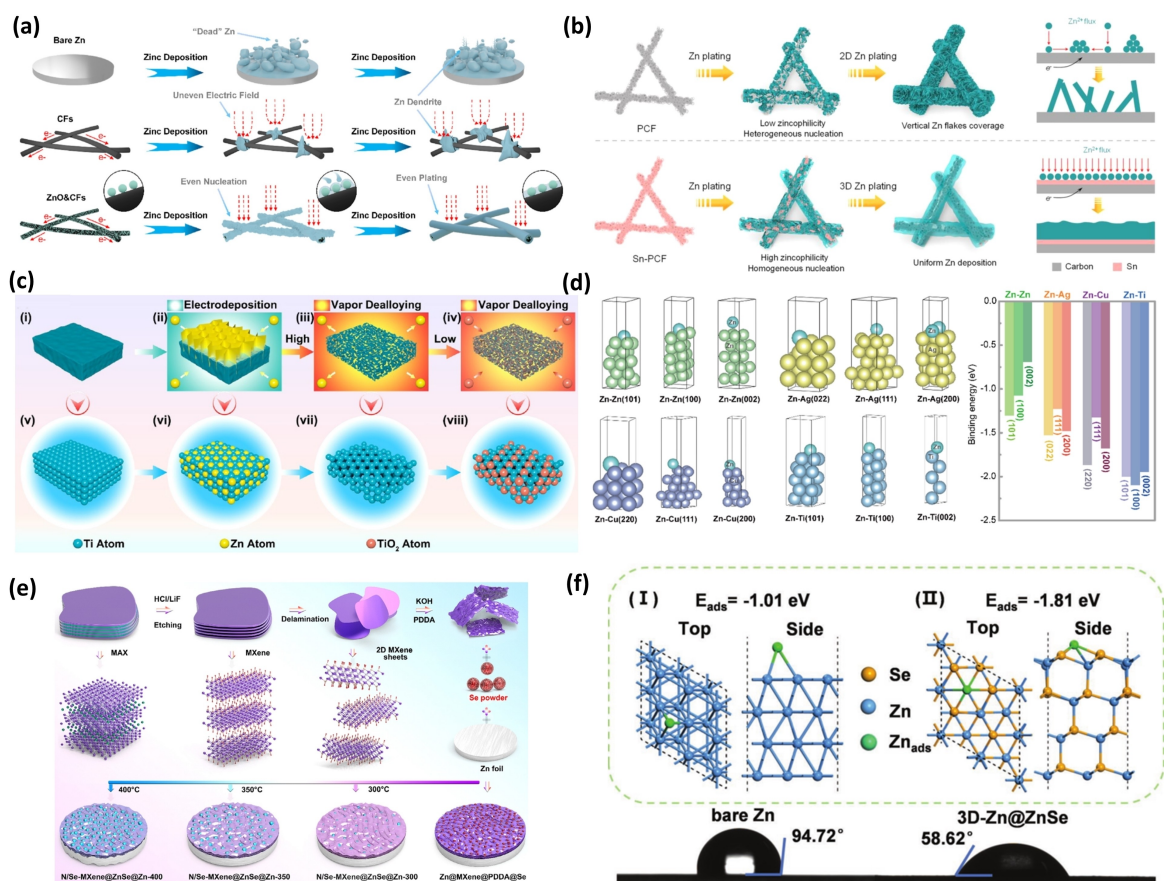


**Figure 4.** a) The plating process of bare Zn, CFs and ZnO&CFs on the surface. Reproduced with permission from Ref. [46]. Copyright (2022) Wiley-VCH. b) The schematic diagrams of Zn deposition on PCF and Sn-PCF. Adapted with permission from Ref. [52]. Copyright (2022) Elsevier B.V. c) The schematic diagram of dealloying process from planar Ti to TiO<sub>2</sub>. Reproduced with permission from Ref. [53]. Copyright (2022) Wiley-VCH. d) The calculated Zn adsorption of Zn, Ag, Cu and Ti metal. Adapted with permission from Ref. [54]. Copyright (2022) Elsevier B.V. e) The schematic diagrams for the preparation of N/Se-MXene@ZnSe film modified Zn foils. Adapted with permission from Ref. [55]. Copyright (2022) Elsevier B.V. f) The optimized adsorption energy of Zn atoms on the bare Zn and the ZnSe substrates. Reproduced with permission from Ref. [56]. Copyright (2022) Wiley-VCH.

sponding polymers. Moreover, zincophilic oxygen/nitrogen dopants can achieve uniform Zn deposition and provide excellent electrochemical performance. Lou et al.<sup>[60]</sup> developed a 3D hybrid fiber body composed of embedded Sn nanoparticles (Sn@NHCf) for Zn metal anodes in high performance Zn metal batteries. Zincophilic Sn nanoparticles with a low nucleation potential and a forceful interaction with Zn<sup>2+</sup> and N-doped carbon ensure homogeneous deposition both on the inner and outer surfaces of the hollow fiber at a low overpotential.

#### 4.2. 3D metal current collectors

Zhang et al.<sup>[53]</sup> designed a reservoir-integrated carbon host (3DP-NC) using zincophilic N,O-functional groups for Zn deposition without dendrite by adjusting the surface binding energy of zinc on the anode. High surface area, high zincophilicity, and abundant nucleation sites were introduced by the interfacial N-doping, resulting in a 3DP-NC host with homogeneous local current distribution and low deposition energy barriers, which greatly promoted homogeneous Zn

nucleation. Feng et al.<sup>[61]</sup> developed an extensible and controllable method for converting commercial Ti foils to 3D porous Ti, the TiO<sub>2</sub> layer enhances the affinity of metallic Zn for the skeleton and promotes uniform Zn metal nucleation (Figure 4c). As a result, zinc-metal anodes with zincophilic 3D current collectors show stable cycling capability with high Coulombic efficiency and long cycles of more than 2000 h. Yu et al.<sup>[62]</sup> designed atomically dispersed Cu (CuZIF-L@TM) in an array of leaf-like Zn-ligated zeolite imidazolium salt backbone (ZIF-L) nanosheets grown on Ti lattices for dendrite-free ZIBs. Due to the highly zincophilicity of Cu single atoms, CuZIF-L@TM can be directly used as the host of anode to guide the deposition of avoiding the carbonation process to prevent structural collapse. In addition, modification of single atoms can maximize the efficiency of atom utilization and thereby induce more uniform nucleation. Chen et al.<sup>[63]</sup> formed a tuned Cu–Zn alloy on a stainless steel mesh to contrast a host of Zn anode. The zincophilic support provides nucleation sites and reduces the energy barrier for axially controlled galvanization. Tuning the Cu/Zn ratio produces a Cu<sub>x</sub>Zn<sub>y</sub> phase that preferentially forms CuZn<sub>5</sub> during the galvanizing process and then converts to metallic zinc during the plating cycle,

which does not decompose during the stripping process at a given voltage range due to the negative Gibbs free energy of forming the zinc alloy. Therefore, regardless of any Cu<sub>x</sub>Zn<sub>y</sub> phase, CuZn<sub>5</sub> is the major zincophilic crystal species in the subsequent cycle, and the Cu–Zn alloy confers an excellent zincophilicity. Dong et al.<sup>[64]</sup> reported a strategy to stabilize zinc anodes using a network of zincophilic Cu nanowires. DFT calculations have shown that the faceted and edge positions of Cu nanowires, in particular the latter, are strongly zincophilic and induce homogeneous nucleation and follow-up deposition of Zn. Huang et al.<sup>[54]</sup> prepared a 3D lightweight silver nanowire aerogel (AgNWA) through a process of self-assembly to direct a homogeneous plating/stripping process (Figure 4d). The combination of DFT calculations and electric field simulations shows that the silver substrate has the best zinc adsorption energy with abundant zincophilic sites, and the 3D structure provides enough space for zinc deposition and reduces the expansion of the zinc anode.

#### 4.3. Other 3D current collectors

Xu et al.<sup>[55]</sup> fabricated *in situ* zincophilic layers consisting of electronically conductive N/Se-doped MXene nanoribbons/nanosheets and ZnSe nanoparticles on zinc foils in a scalable manner (Figure 4e). While the process of selenization, the functionalization of N/Se and the formation of ZnSe nanoparticle were achieved simultaneously by a simple vacuum annealing method. The ZnSe nanoparticles formed simultaneously can provide an abundant number of zincophilic sites and enhance the reversibility of batteries. Zhi et al.<sup>[56]</sup> introduced a 3D Zn conducting framework with a strongly zincophilic ZnSe layer on the surface of anode through a single step constant potential sweep, and the internal cavity of the 3D collector formed by electrooxidation was utilized as the site of zinc plating, greatly reduced current density and enhanced nucleation sites (Figure 4f). DFT calculations demonstrated that the electrodeposited ZnSe layer enhances the zincophilicity and lowers the desolvation energy barrier. Thus, electrochemical pretreatment enables precise targeting and removal of the Zn foil protrusions for roughened commercial Zn foils, which are mostly used as sites for building of dendrite as well as side reactions.

However, due to the high melting point of zinc,<sup>[8]</sup> researchers often deposit Zn into a three-dimensional current collectors by electrodeposition. Electrodeposition in a three-electrode system often results in loosely arranged and lattice anisotropic zinc, which is not conducive to subsequent uniform deposition. At the same time, large areal capacity and high current density are the key indicators to evaluate the performance of ZIBs in practical applications. There are still few reports on the use of three-dimensional current collectors as the host of zinc anode under high current density and large areal capacity. Therefore, how to overcome this problem in practical applications still needs further exploration by researchers.

## 5. Electrolyte Engineering

The electrolyte is an important component of the batteries,<sup>[65]</sup> which renders as an ion conductor, providing ion transport between the cathode and anode, which plays a key role in the electrochemical performance of the batteries.

#### 5.1. In situ reaction to form zincophilic SEI

The establishment of zincophilic sites on anode substrates is a valid method to restrain zinc dendrite. The strategy is attributed to the tendency of Zn<sup>2+</sup> ions to combine with zincophilic sites to distribute nucleation sites, so as to deposit evenly. However, the high cost of the host material and the harsh preparation conditions undoubtedly reduce practicability of this strategy. In practical terms, the construction of zincophilic sites on the surface of zinc anode by electrolyte additives is expected to be an ideal way to achieve even zinc growth.

Zhu et al.<sup>[66]</sup> used filamentous protein (SF) as an additive of electrolyte, the SF additive is able to preferably adsorb on the zinc surface and *in situ* react to produce a polymer coating (Figure 5a). Because of the substantial polar groups, the polymer coating has highly zincophilicity, which promotes Zn<sup>2+</sup> flux, directs uniform redistribution of Zn<sup>2+</sup>, and inhibits the growth of dendrite. Xu et al.<sup>[67]</sup> built dense and uniform ZnO@Cu protected interfacial layer with highly zincophilicity by TS electrolyte additive on the zinc anode (Figure 5b), which enhances the electrochemical stability of the zinc anode and insulates the anode from the electrolyte to prevent hydrogen evolution. Furthermore, the zincophilic ZnO@Cu interfacial layer can provide zinc ion nucleation sites, greatly inhibit the formation of zinc dendrites, and improve the electrochemical performance of zinc anode.

#### 5.2. Adsorption of zincophilic additives on the surface of anode

Lu et al.<sup>[68]</sup> proposed zincophilic Lewis base N,N-dimethylformamide (DMF) containing a large amount of unshared para electrons as a great electrolyte additive for deposition of zinc without dendrite even under harsh conditions (Figure 5c). Due to the zincophilic property of DMF, the Zn<sup>2+</sup> solvated structure will be modified by promoting the binding of Zn<sup>2+</sup> with DMF and OTf. DMF on the zinc metal surface adsorption energy ( $-0.579$  eV) is higher than that of free H<sub>2</sub>O ( $-0.251$  eV). In addition, it tests the zincophilicity of the unshared para electron-containing solvent, weakening the solvated structure of Lewis acidic Zn<sup>2+</sup>, replacement of some interface-adsorbed H<sub>2</sub>O molecules, homogenization of Zn<sup>2+</sup> nucleation, and inhibition of side reactions related by electrolyte. Zhu et al.<sup>[69]</sup> proposed a low cost and environmentally friendly additive, nettle extract (NE), to direct uniform Zn deposition through designed *in situ* zincophilic sites (Figure 5d). Through experimental characterization and DFT calculation, the zinco-

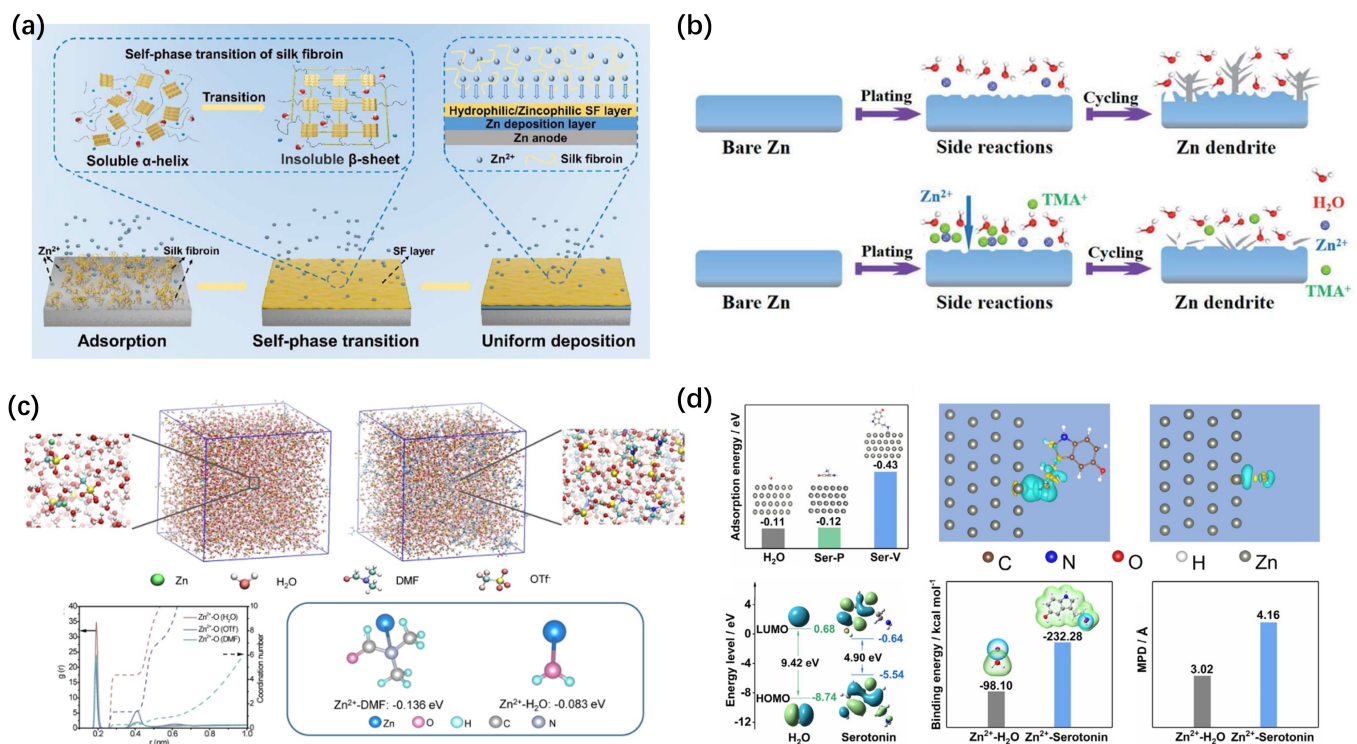


**Figure 5.** a) Diagrammatic sketch of the self-phase transition of SF polymeric layer on the surface of zinc anode. Adapted with permission from Ref. [66]. Copyright (2022) Elsevier B.V. b) A sketch map of Zn deposition on Zn metal in 2 M  $ZnSO_4$  with/without TS. Reproduced with permission from Ref. [67]. Copyright (2022) Royal Society of Chemistry. c) The results of MD Simulation results for ZOTF and ZOTF-2H1D electrolytes. Reproduced with permission from Ref. [68]. Copyright (2022) Wiley-VCH. d) DFT calculate the mechanism of NE in ZIBs. Adapted with permission from Ref. [69]. Copyright (2022) Elsevier B.V.

philic NE is adsorbed on the Zn surface to provide a more efficient site for zinc nucleation, thus effectively inhibiting the generation of dendrites. The symmetric cell containing NE has stable cycles for over 2200 h at 5 mA cm $^{-2}$ . Zincophilic di-2-pyridylamine (DPA) achieve long cycles for zinc anodes under severe cycling conditions by Zhu et al.<sup>[70]</sup> The DPA molecule is able to prior adsorb to the Zn surface due to its super zincophilicity, which tightly regulates the random Zn $^{2+}$  diffusion. Therefore, the interface of anode/electrolyte was stabilized and highly reversible plating/stripping was ultimately achieved even under high current densities. Polyamino acids (PAA) were used as multifunctional electrolyte additives for modified zinc anode. The DFT calculations have showed that PAA has a unique long-chain structure, abundant nitrogen and oxygen functional groups and highly zincophilicity through preferential absorption by Wang et al.<sup>[71]</sup> As a result, PAA can be tightly adsorbed on the surface of the Zn anode to construct a hydrophilic artificial coating. Four models were developed to study the interaction between the Zn foil and other components of the electrolyte, including PAA, AA, H $_2$ O and Zn ions. The adsorption energies of PAA, AA and Zn ions on the Zn surface were got to be -2.22 eV, -0.77 eV and -0.83 eV, respectively. Compared with Zn ion, PAA has much higher binding energy to Zn electrode, so a homogeneous protective layer is applied on the surface of Zn to inhibit the side reaction. Furthermore, the binding energy of PAA with Zn is larger than that of H $_2$ O (0.29 eV), which isolates the adsorption of water to prevent the precipitation of hydrogen. In addition to being

able to absorb on the Zn foil, MXene additive can guide homogeneous initial Zn deposition by providing massive zincophilic oxygen functional groups. The functional layer uniform the Zn $^{2+}$  dispersion on the surface and provides well-dispersed sites to induce uniform nucleation during deposition and uniform ion flux during deposition, thereby inhibiting the growth of Zn dendrites.<sup>[72]</sup>

### 5.3. Other electrolyte engineering

In addition to the construction of SEI on the surface of zinc anode through electrolyte and additives, ionic liquids and deep eutectic solvents are also excellent strategies to enhance the zincophilicity of the interface between anode and electrolyte.<sup>[68,73-75]</sup> Ilyas et al.<sup>[73]</sup> prepared intrinsically safe electrolyte by combining ionic liquid 3-dodecyl-1-vinylimidazolium hexafluorophosphate with triethyl phosphate TEP or trimethyl phosphate TMP. Ionic liquids provide zincophilic sites containing N and F elements. The combination of zinc ions with their sites significantly enhances the transport of Zn $^{2+}$  and promotes the uniform deposition of zinc. A hydrated eutectic electrolyte system containing methanesulfonyl methane, zinc perchlorate and water was prepared by Han et al.<sup>[74]</sup> The strong coordination interaction between Zn $^{2+}$  and methanesulfonyl methane resulted in additional desolvation barrier, enhanced the diffusion kinetics of zinc ions, and promoted the non-dendritic deposition of zinc.

## 6. Separator Modification

The separator has a major influence on the safety of the battery. It plays a role in isolating the anode and cathode, avoiding direct contact between electrodes, preventing short circuit.<sup>[76]</sup> The modification of separator surface coating and the construction of functional zincophilic separator are effective technologies to enhance the electrochemical performance of zinc-ion batteries.

Feng et al.<sup>[77]</sup> designed a freestanding, lightweight and zincophilic separator of MXene/nanoporous oxide heterostructures to stabilize Zn metal anodes. The zincophilic MXene@oxides layer can uniform the electric field distribution to modulate Zn deposition, reducing the nucleation overpotential for Zn deposition, as well as promoting ion transport by reducing the  $Zn^{2+}$  concentration gradient to further induce homogenize Zn deposition and suppress side reactions. Due to the superiority of the designed spacers, the reversibility and stability of the zinc metal anode was excellent without dendrites. Kim et al.<sup>[78]</sup> proposed that the large pore sizes of GF separators are capable of accommodating large numbers of aqueous electrolytes. The silicate fibers have a highly zincophi-

licity and facilitates the transport of the Zn ions. The GF separator induces a restricted Zn deposition, prevents Zn dendrites from perforating the diaphragm, and enhances the stability of cell cycling.

Wu et al.<sup>[79]</sup> developed a functional separator consisting of cellulose nanofibers and graphene oxide (CG) for stable Zn ion batteries without dendrites (Figure 6a), obtained by manipulating uniform hexagonal Zn deposits in the (002) crystallographic plane direction. There is a strong interaction between the negative charge on the surface of the CG separator and the abundant zincophilic oxygen functional groups to induce uniform zinc deposition. Janus separators were developed by directly growing vertical graphene (VG) on one side of a commercial glass fiber separator throughout the entire CVD process by Sun et al.<sup>[80]</sup> (Figure 6b). The oxygen and nitrogen heteroatoms were successfully bonded to bare graphene by a simple air plasma treatment. The oxygen and nitrogen heteroatoms were successfully bonded to bare graphene through simple air plasma treatment. This Janus separator can achieve uniform electric field distribution, reducing the local current density at the anode/electrolyte interface, and using

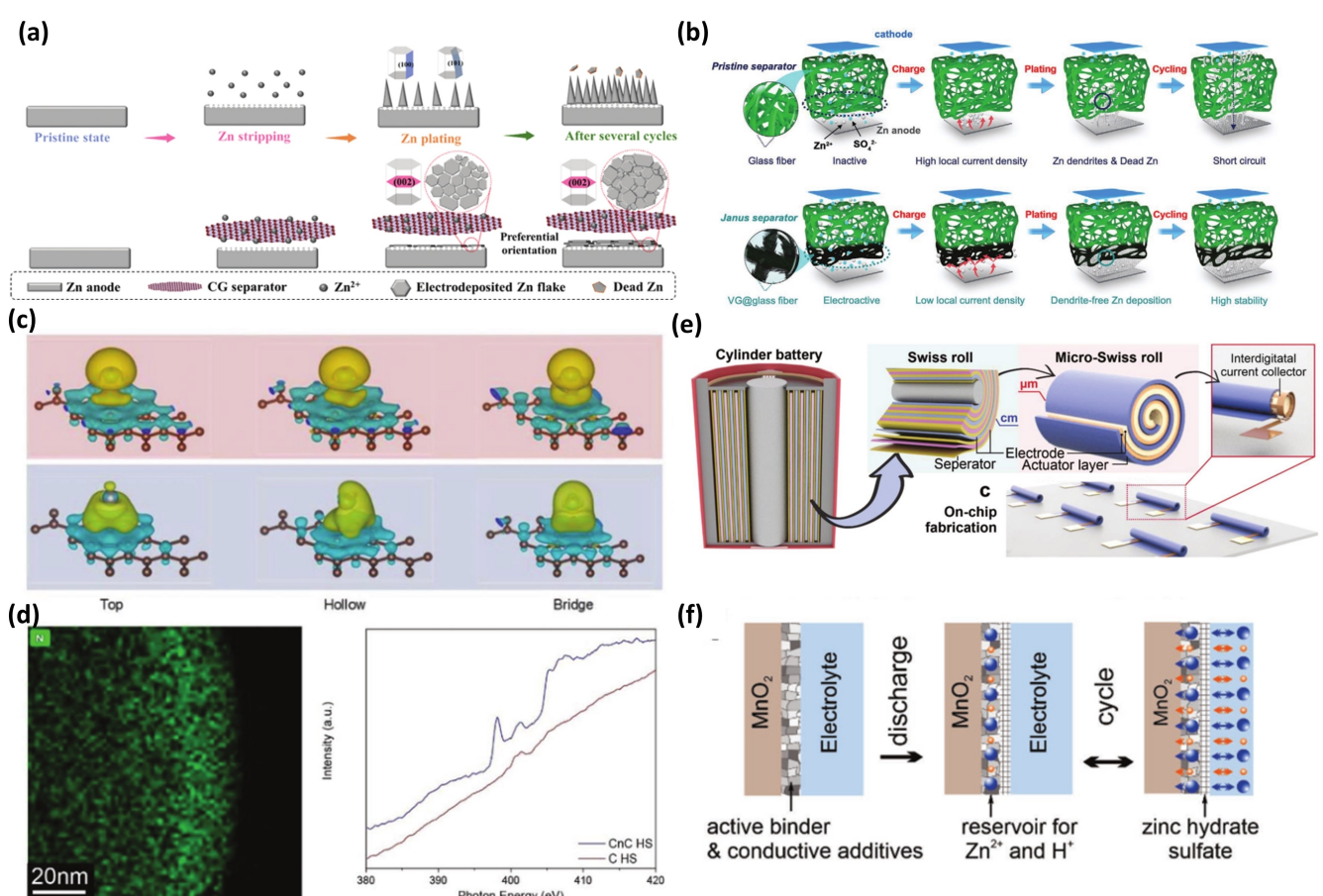


**Figure 6.** a) Schematic representation of the deposition processes of zinc with different separator. Reproduced with permission from Ref. [79]. Copyright (2021) Wiley-VCH. b) Schematics illustration of the VG Janus separator. Reproduced with permission from Ref. [80]. Copyright (2020) Wiley-VCH. c) The charge difference of various adsorption sites between graphene/N-doped graphene and Zn. d) Elemental mapping and NEXAFS of the nitrogen content. Reproduced with permission from Ref. [81]. Copyright (2021) Wiley-VCH. e) The concept and realization of Swiss rolls and micro-Swiss roll in batteries. f) Schematic illustration of the electrode-electrolyte interface function induced by PI. Reproduced with permission from Ref. [82]. Copyright (2022) Wiley-VCH.

the zincophilicity of oxygen and nitrogen functional groups to uniform the zinc ion flux and induce uniform zinc deposition.

Wang et al.<sup>[83]</sup> constructed a single diaphragm decorated with functional supramolecules (GF@SM) to guide uniform zinc ion distribution and enhance the electrochemical performance of zinc metal anodes. Zincophilic groups (amino, carbonyl and triazine) in the supramolecule were found to have excellent zincophilicity, preventing Zn ions from accumulating on the electrode surface, and migrating zinc ions would be well induced to deposit a uniform manner inhibiting the formation of dendrites. Zhang<sup>[84]</sup> stabilized the zinc metal anode by sputtering Sn magnetron on the separator. The highly conductive and highly zincophilicity Sn coating helps to homogenize the  $Zn^{2+}$  solder while also controlling the direction of Zn metal growth.

## 7. Techniques

Qiao et al.<sup>[81]</sup> reported an exhaustive investigation of the mechanism of the zincophilic site on the basis of various *in situ/ex situ* techniques (Figure 6c). The host used carbon with nitrogen functional group as a zincophilic site, *in situ* near-edge X-ray absorption fine structure (NEXAFS) and *in situ* Raman spectroscopy were used in exploring ZIBs (Figure 6d). The results show that Zn–N bonds are forming by  $Zn^{2+}$  and pyridine, the Zn–N bonds induced a large number of zinc nucleation on the host while inhibited zinc dendrites. In addition to improved electrochemical properties, hosts with zincophilic sites exhibit uniform zinc deposition of Zn. Schmidt et al.<sup>[82]</sup> developed an on-chip Swiss coil current collector fabricated by a miniaturization process and injected with a manganese dioxide slurry consisting of a zincophilic binder (Figure 6e, f). The zincophilic binder layer enhanced the transport of zinc ions and inhibited the dissolution of manganese dioxide. Guan et al.<sup>[85]</sup> reported a zincophilic zinc foil with three-dimensional micropatterns using a simple and scalable imprinting strategy using a pre-designed mold with a femtosecond laser. The imprint-induced microchannels with enhanced  $Zn^{2+}$  affinity not only effectively regulate the concentration distribution of  $Zn^{2+}$  ions, but also prevent short-circuiting of vertical dendrite growth, achieving a unique microchannel-induced spatially selective deposition behavior. This simple imprinting technique can be easily scaled up and effectively extended to other zincophilic materials. Ding et al.<sup>[86]</sup> adapted a metallurgical surface finishing method to manufacture patterned zinc anodes with periodic concave and convex shapes from commercially available zinc metal. Laser lithography is a mature industrial process for metal surface modification, additive manufacturing and micromachining. But it has never been used to design the host structure of zinc metal anode and it has a great prospect in the expandable manufacturing and industrial practicability of zinc electrode. LLP@ZF has been proven to include chemically induced zincophilicity at the surface as well as geometrically induced hydrophilicity. The combination of these two properties

enables simple and cycle-stable metal anode plating/stripping kinetics and full cell performance.

## 8. Zincophilicity-zincophobicity combination design

Typically, the zincophilic interface reduces the nucleation barrier and zinc metal can improve the homogeneity of zinc deposition by constructing a stable structure with zincophilic sites. The zincophobic interface can also regulate the initial nucleation and inhibit the subsequent Zn dendrites because of its certain degree of inhibition of rapid ion migration and shielding effect on hydrated zinc ions in the electrolyte.<sup>[87,88]</sup>

A concept of layered constraint to balance the advantages of zincophilic sites and the additional problems which brings, and embeds a large number of porous zincophilic Co in the carbon cage to design a hierarchical limited zinc anode host was proposed by Chao et al.<sup>[89]</sup> As a preferential nucleation site with low nucleation potential, the zincophilic Co site induces uniform zinc deposition. The carbon cage further restricts the deposition of zinc in three-dimensional space. This strategy can achieve more than 800 stable cycles of the battery at a high current density of  $20\text{ mA cm}^{-2}$ .

Wang et al.<sup>[90]</sup> overcame the two challenges of the growth of zinc dendrites and poor performance at low-temperature by using a eutectic 7.6 m  $ZnCl_2$  aqueous electrolyte containing 0.05 m  $SnCl_2$  additive, resulting in the formation of a zincophilic/zincophobic  $Sn/Zn_5(OH)_8Cl_2-H_2O$  double-layer interface. The zincophilic Sn reduces the overpotential during Zn plating/stripping and accelerates homogenize Zn deposition, while the zincophobicity  $Zn_5(OH)_8Cl_2-H_2O$  center point top layer inhibits the growth of zinc dendrites. For the  $Zn||Ti$  half-cell, the eutectic electrolyte has a high coulombic efficiency in excess of 99.7% over 200 cycles.

## 9. Conclusion and Prospect

Zinophilic designs with high binding energy can provide a lower nucleation potential to promote the kinetics of Zn deposition, and therefore, zinc nucleation is more likely to occur at zincophilic sites. Although the introduction of zincophilic sites can solve the kinetics problem to some extent, the inhomogeneous distribution of zincophilic sites, agglomeration or site coverage problems brought about by compounding with Zn will undoubtedly lead to the loss of induced functionality, resulting in inhomogeneous Zn deposition or dendrite generation during the cycle. It deserves attention that the greater the zincophilic nature of the modified layer is not necessarily the better, but needs to be taken into account. As the capacity of zinc deposition increases, it may exceed the zinc control capacity of the zincophilic sites, and zinc dendrites will still be formed at this time, while the restricted deposition space below the poorly zincophilic modified layer can further mechanically inhibit large-scale dendrite growth. In contrast,

the surface of the highly zincophilic modified layer no longer has a restraining effect, and the cell is more easily damaged by dendrites. Therefore, how to balance the zincophilicity/zincophobicity properties of the interfacial layer is a key challenge for the future development of ZIBs.

In this review, several factors affect the zincophilicity of the interface of electrode/electrolyte, including surface energy and chemical interactions. Problems and strategies to improve the zincophilicity of different interfaces of electrode/electrolyte are also discussed. This review is conducive to elucidate the understanding of the interfacial chemistry of various electrolytes with zinc metal and guides the practical application of interfacial engineering to achieve promising rechargeable batteries.

## Acknowledgements

This work was supported by the National Natural Science Foundation of China (No. 22078078), the Natural Science Foundation of Heilongjiang Province (No. LH2020B008), State Key Laboratory of Urban Water Resource and Environment (Harbin Institute of Technology)(No . 2022TS20)

## Conflict of Interest

The authors declare no competing interests.

**Keywords:** aqueous zinc-ion batteries • electrode/electrolyte interface • zincophilicity

- [1] W. Cao, Q. Li, X. Yu, H. Li, *eScience* **2022**, *2*, 47–78.
- [2] F. Wang, O. Borodin, T. Gao, X. Fan, W. Sun, F. Han, A. Faraone, J. A. Dura, K. Xu, C. Wang, *Nat. Mater.* **2018**, *17*, 543–549.
- [3] N. Liu, X. Wu, L. Fan, S. Gong, Z. Guo, A. Chen, C. Zhao, Y. Mao, N. Zhang, K. Sun, *Adv. Mater.* **2020**, *32*, 1908420.
- [4] H. Lu, X. Zhang, M. Luo, K. Cao, Y. Lu, B. Xu, H. Pan, K. Tao, Y. Jiang, *Adv. Funct. Mater.* **2021**, *31*, 2103514.
- [5] Z. Pei, *Nano Res. Energy* **2022**, *1*, e9120023.
- [6] D. Lin, Y. Liu, Z. Liang, H. W. Lee, J. Sun, H. Wang, K. Yan, J. Xie, Y. Cui, *Nat. Nanotechnol.* **2016**, *11*, 626–632.
- [7] M. Liu, L. Yang, H. Liu, A. Amine, Q. Zhao, Y. Song, J. Yang, K. Wang, F. Pan, *ACS Appl. Mater. Interfaces* **2019**, *11*, 32046–32051.
- [8] V. Kuklik, J. Kudláček, *Hot-Dip Galvanizing of Steel Structures* **2016**, 133–143.
- [9] L. Zhou, F. Yang, S. Zeng, X. Gao, X. Liu, X. Cao, P. Yu, X. Lu, *Adv. Funct. Mater.* **2021**, *32*, 2110829.
- [10] Y. Zeng, P. X. Sun, Z. Pei, Q. Jin, X. Zhang, L. Yu, X. W. D. Lou, *Adv. Mater.* **2022**, *34*, 2200342.
- [11] M. Kwon, J. Lee, S. Ko, G. Lim, S.-H. Yu, J. Hong, M. Lee, *Energy Environ. Sci.* **2022**, *15*, 2889–2899.
- [12] H. Meng, Q. Ran, T. Y. Dai, H. Shi, S. P. Zeng, Y. F. Zhu, Z. Wen, W. Zhang, X. Y. Lang, W. T. Zheng, Q. Jiang, *Nano-Micro Lett.* **2022**, *14*, 128.
- [13] L. Hong, L. Y. Wang, Y. Wang, X. Wu, W. Huang, Y. Zhou, K. X. Wang, J. S. Chen, *Adv. Sci.* **2022**, *9*, e2104866.
- [14] Y. Tian, Y. An, C. Liu, S. Xiong, J. Feng, Y. Qian, *Energy Storage Mater.* **2021**, *41*, 343–353.
- [15] Y. Tian, S. Chen, Y. He, Q. Chen, L. Zhang, J. Zhang, *Nano Res. Energy* **2022**, *1*, e9120025.
- [16] M. Wang, Y. Meng, K. Li, T. Ahmad, N. Chen, Y. Xu, J. Sun, M. Chuai, X. Zheng, Y. Yuan, C. Shen, Z. Zhang, W. Chen, *eScience* **2022**, *2*, 509–517.
- [17] T. Foroozan, V. Yurkiv, S. Sharifi-Asl, R. Rojaee, F. Mashayek, R. Shahbazian-Yassar, *ACS Appl. Mater. Interfaces* **2019**, *11*, 44077–44089.
- [18] G. Chen, Z. Sang, J. Cheng, S. Tan, Z. Yi, X. Zhang, W. Si, Y. Yin, J. Liang, F. Hou, *Energy Storage Mater.* **2022**, *50*, 589–597.
- [19] B. Jiang, W. Liu, Z. Ren, R. Guo, Y. Huang, C. Xu, F. Kang, *Front. Chem.* **2022**, *10*, 899810.
- [20] C. Zhao, Y. Du, Z. Guo, A. Chen, N. Liu, X. Lu, L. Fan, Y. Zhang, N. Zhang, *Energy Storage Mater.* **2022**, *53*, 322–330.
- [21] X. Lu, C. Zhao, A. Chen, Z. Guo, N. Liu, L. Fan, J. Sun, N. Zhang, *Chem. Eng. J.* **2023**, *451*, 138772.
- [22] Z. Guo, L. Fan, C. Zhao, A. Chen, N. Liu, Y. Zhang, N. Zhang, *Adv. Mater.* **2022**, *34*, 2105133.
- [23] A. Chen, C. Zhao, Z. Guo, X. Lu, N. Liu, Y. Zhang, L. Fan, N. Zhang, *Energy Storage Mater.* **2022**, *44*, 353–359.
- [24] H. Wang, Y. Chen, H. Yu, W. Liu, G. Kuang, L. Mei, Z. Wu, W. Wei, X. Ji, B. Qu, L. Chen, *Adv. Funct. Mater.* **2022**, *32*, 2205600.
- [25] J. Zhou, M. Xie, F. Wu, Y. Mei, Y. Hao, R. Huang, G. Wei, A. Liu, L. Li, R. Chen, *Adv. Mater.* **2021**, *33*, 2101649.
- [26] N. Naresh, S. Eom, S. Hwan Jeong, S. Jun Lee, S. Hyeon Park, J. Park, J.-H. Ahn, J.-H. Kim, Y. Hwa Jung, *Appl. Surf. Sci.* **2022**, *606*, 154932.
- [27] S. Kim, U. Hwang, K. Yang, M. Cho, J.-D. Nam, Y. Lee, *Chem. Eng. J.* **2022**, *440*, 135822.
- [28] L. Tan, C. Wei, Y. Zhang, Y. An, S. Xiong, J. Feng, *Chem. Eng. J.* **2022**, *431*, 134277.
- [29] X. Zhu, X. Li, M. L. K. Essandoh, J. Tan, Z. Cao, X. Zhang, P. Dong, P. M. Ajayan, M. Ye, J. Shen, *Energy Storage Mater.* **2022**, *50*, 243–251.
- [30] Z. Pan, Q. Cao, W. Gong, J. Yang, Y. Gao, Y. Gao, J. Pu, J. Sun, X. J. Loh, Z. Liu, C. Guan, J. Wang, *Energy Storage Mater.* **2022**, *50*, 435–443.
- [31] G. Li, X. Wang, S. Lv, J. Wang, X. Dong, D. Liu, *Chem. Eng. J.* **2022**, *450*, 138116.
- [32] N. Hu, H. Qin, X. Chen, Y. Huang, J. Xu, H. He, *Front. Chem.* **2022**, *10*, 981623.
- [33] T. C. Li, Y. V. Lim, X. Xie, X. L. Li, G. Li, D. Fang, Y. Li, Y. S. Ang, L. K. Ang, H. Y. Yang, *Small* **2021**, *17*, e2101728.
- [34] J.-Q. Huang, Z. Hou, P. Gao, X. Yan, X. Lin, B. Zhang, *Mater. Today Commun.* **2022**, *32*, 103939.
- [35] C. Peng, Y. Zhang, S. Yang, L.-L. Zhang, Z. Wang, *Nano Energy* **2022**, *98*, 107329.
- [36] C. Wang, Y. Gao, L. Sun, Y. Zhao, D. Yin, H. Wang, J. Cao, Y. Cheng, L. Wang, *Nano Res.* **2022**, *15*, 8076–8082.
- [37] M. He, C. Shu, A. Hu, R. Zheng, M. Li, Z. Ran, J. Long, *Energy Storage Mater.* **2022**, *44*, 452–460.
- [38] L. Yuan, J. Xu, Z. Yang, Q. Su, J. Li, *J. Power Sources* **2022**, *517*, 230696.
- [39] H. Fan, M. Li, E. Wang, *Nano Energy* **2022**, *103*, 107751.
- [40] C. Guo, J. Zhou, Y. Chen, H. Zhuang, Q. Li, J. Li, X. Tian, Y. Zhang, X. Yao, Y. Chen, S. L. Li, Y. Q. Lan, *Angew. Chem. Int. Ed.* **2022**, *61*, e202210871.
- [41] J. Zhao, Y. Ying, G. Wang, K. Hu, Y. D. Yuan, H. Ye, Z. Liu, J. Y. Lee, D. Zhao, *Energy Storage Mater.* **2022**, *48*, 82–89.
- [42] F. Wang, H. Lu, H. Li, J. Li, L. Wang, D. Han, J. Gao, C. Geng, C. Cui, Z. Zhang, Z. Weng, C. Yang, J. Lu, F. Kang, Q.-H. Yang, *Energy Storage Mater.* **2022**, *50*, 641–647.
- [43] J. L. Yang, J. Li, J. W. Zhao, K. Liu, P. Yang, H. J. Fan, *Adv. Mater.* **2022**, *2202382*.
- [44] H. Liu, J.-G. Wang, W. Hua, L. Ren, H. Sun, Z. Hou, Y. Huyan, Y. Cao, C. Wei, F. Kang, *Energy Environ. Sci.* **2022**, *15*, 1872–1881.
- [45] Z. Zhang, R. Wang, J. Hu, M. Li, K. Wang, K. Jiang, *Sustain. Energy Fuels* **2021**, *5*, 5843–5850.
- [46] H. W. Kim, J. U. Jin, D. Lee, S. G. Kim, B. C. Ku, S. Ryu, N. H. You, *Int. J. Energy Res.* **2022**, *46*, 16918–16928.
- [47] R. Wang, L. Wu, Y. Wei, K. Zhu, H. Wang, Y. Yao, *Mater. Today Energy* **2022**, *29*, 101097.
- [48] P. Xue, C. Guo, N. Wang, K. Zhu, S. Jing, S. Kong, X. Zhang, L. Li, H. Li, Y. Feng, W. Gong, Q. Li, *Adv. Funct. Mater.* **2021**, *31*, 2106417.
- [49] Q. Guan, Y. Li, X. Bi, J. Yang, J. Zhou, X. Li, J. Cheng, Z. Wang, B. Wang, J. Lu, *Adv. Energy Mater.* **2019**, *9*, 1901434.
- [50] J. Zhou, M. Xie, F. Wu, Y. Mei, Y. Hao, L. Li, R. Chen, *Adv. Mater.* **2022**, *34*, 2106897.
- [51] P. X. Sun, Z. Cao, Y. X. Zeng, W. W. Xie, N. W. Li, D. Luan, S. Yang, L. Yu, X. W. D. Lou, *Angew. Chem. Int. Ed.* **2022**, *61*, e202115649.
- [52] J.-L. Yang, P. Yang, W. Yan, J.-W. Zhao, H. J. Fan, *Energy Storage Mater.* **2022**, *51*, 259–265.
- [53] L. Zeng, H. He, H. Chen, D. Luo, J. He, C. Zhang, *Adv. Energy Mater.* **2022**, *12*, 2103708.
- [54] W. Ling, Q. Yang, F. Mo, H. Lei, J. Wang, Y. Jiao, Y. Qiu, T. Chen, Y. Huang, *Energy Storage Mater.* **2022**, *51*, 453–464.

- [55] Y. Tian, Y. An, Y. Yang, B. Xu, *Energy Storage Mater.* **2022**, *49*, 122–134.
- [56] Z. Bie, Q. Yang, X. Cai, Z. Chen, Z. Jiao, J. Zhu, Z. Li, J. Liu, W. Song, C. Zhi, *Adv. Energy Mater.* **2022**, 2202683.
- [57] J. Li, S. Zhang, Y. Wu, B. Jin, M. Shao, *Mater. Today Energy* **2021**, *22*, 100849.
- [58] J. Zhao, Z. Cong, J. Hu, H. Lu, L. Wang, H. Wang, O. I. Malyi, X. Pu, Y. Zhang, H. Shao, Y. Tang, Z. L. Wang, *Nano Energy* **2022**, *93*, 106893.
- [59] Z. Xu, S. Jin, N. Zhang, W. Deng, M. H. Seo, X. Wang, *Nano Lett.* **2022**, *22*, 1350–1357.
- [60] Y.-X. Z. H. Yu, N.-W. Li, D.-Y. Luan, L. Yu, X.-W. Lou, *Sci. Adv.* **2022**, *8*, eabm5766.
- [61] Y. An, Y. Tian, S. Xiong, J. Feng, Y. Qian, *ACS Nano* **2021**, *15*, 11828–11842.
- [62] Y. Tao, S. W. Zuo, S. H. Xiao, P. X. Sun, N. W. Li, J. S. Chen, H. B. Zhang, L. Yu, *Small* **2022**, *18*, e2203231.
- [63] Q. Zhao, Y. Wang, W. Liu, X. Liu, H. Wang, H. Yu, Y. Chen, L. Chen, *Adv. Mater. Interfaces* **2022**, *9*, 2102254.
- [64] S. Xie, Y. Li, X. Li, Y. Zhou, Z. Dang, J. Rong, L. Dong, *Nano-Micro Lett.* **2021**, *14*, 39.
- [65] Z. Tang, H. Wang, P. F. Wu, S. Y. Zhou, Y. C. Huang, R. Zhang, D. Sun, Y. G. Tang, H. Y. Wang, *Angew. Chem. Int. Ed.* **2022**, *61*, e202200475.
- [66] L. Zhang, T. Zhang, W. Xin, H. Peng, Z. Yan, Z. Zhu, *Mater. Today Energy* **2022**, *29*, 101130.
- [67] Q. Hu, J. Hu, Y. Li, X. Zhou, S. Ding, Q. Zheng, D. Lin, J. Zhao, B. Xu, *J. Mater. Chem. A* **2022**, *10*, 11288–11297.
- [68] L. Zhou, F. Wang, F. Yang, X. Liu, Y. Yu, D. Zheng, X. Lu, *Angew. Chem. Int. Ed.* **2022**, *61*, e202208051.
- [69] L. Zhang, L. Miao, W. Xin, H. Peng, Z. Yan, Z. Zhu, *Energy Storage Mater.* **2022**, *44*, 408–415.
- [70] Y. Geng, L. Miao, Z. Yan, W. Xin, L. Zhang, H. Peng, J. Li, Z. Zhu, *J. Mater. Chem. A* **2022**, *10*, 10132–10138.
- [71] J. Liu, W. Song, Y. Wang, S. Wang, T. Zhang, Y. Cao, S. Zhang, C. Xu, Y. Shi, J. Niu, F. Wang, *J. Mater. Chem. A* **2022**, *10*, 20779–20786.
- [72] C. Sun, C. Wu, X. Gu, C. Wang, Q. Wang, *Nano-Micro Lett.* **2021**, *13*, 89.
- [73] F. Ilyas, J. Chen, Y. Zhang, H. Lu, Y. Huang, H. Ma, J. Wang, *Angew. Chem. Int. Ed.* **2023**, *62*, e202215110.
- [74] M. Han, J. Huang, X. Xie, T. C. Li, J. Huang, S. Liang, J. Zhou, H. J. Fan, *Adv. Funct. Mater.* **2022**, *32*.
- [75] L. Geng, J. Meng, X. Wang, C. Han, K. Han, Z. Xiao, M. Huang, P. Xu, L. Zhang, L. Zhou, L. Mai, *Angew. Chem. Int. Ed.* **2022**, *61*, e202206717.
- [76] Y. Zhang, X. Li, L. Fan, Y. Shuai, N. Zhang, *Cell Rep.* **2022**, *3*, 100824.
- [77] Y. An, Y. Tian, Q. Man, H. Shen, C. Liu, Y. Qian, S. Xiong, J. Feng, Y. Qian, *ACS Nano* **2022**, *16*, 6755–6770.
- [78] R. Kim, J. Jung, J.-H. Lee, S. Kim, J. Heo, K. Shin, J. Kim, H.-T. Kim, *ACS Sustainable Chem. Eng.* **2021**, *9*, 12242–12251.
- [79] J. Cao, D. Zhang, C. Gu, X. Wang, S. Wang, X. Zhang, J. Qin, Z. S. Wu, *Adv. Energy Mater.* **2021**, *11*, 2101299.
- [80] C. Li, Z. Sun, T. Yang, L. Yu, N. Wei, Z. Tian, J. Cai, J. Lv, Y. Shao, M. H. Rummeli, J. Sun, Z. Liu, *Adv. Mater.* **2020**, *32*, 2003425.
- [81] F. Xie, H. Li, X. Wang, X. Zhi, D. Chao, K. Davey, S. Z. Qiao, *Adv. Energy Mater.* **2021**, *11*, 2003419.
- [82] Z. Qu, M. Zhu, Y. Yin, Y. Huang, H. Tang, J. Ge, Y. Li, D. D. Karnaushenko, D. Karnaushenko, O. G. Schmidt, *Adv. Energy Mater.* **2022**, *12*, 2200714.
- [83] T. Liu, J. Hong, J. Wang, Y. Xu, Y. Wang, *Energy Storage Mater.* **2022**, *45*, 1074–1083.
- [84] Z. Hou, Y. Gao, H. Tan, B. Zhang, *Nat. Commun.* **2021**, *12*, 3083.
- [85] Q. Cao, Z. Pan, Y. Gao, J. Pu, G. Fu, G. Cheng, C. Guan, *Adv. Funct. Mater.* **2022**, *32*, 2205771.
- [86] Z. Huang, H. Li, Z. Yang, H. Wang, J. Ding, L. Xu, Y. Tian, D. Mitlin, J. Ding, W. Hu, *Energy Storage Mater.* **2022**, *51*, 273–285.
- [87] W. Li, Q. Zhang, Z. Yang, H. Ji, T. Wu, H. Wang, Z. Cai, C. Xie, Y. Li, H. Wang, *Small* **2022**, e2205667.
- [88] C. Xie, Q. Zhang, Z. Yang, H. Ji, Y. Li, H. Li, L. Fu, D. Huang, Y. Tang, H. Wang, *Chin. Chem. Lett.* **2022**, *33*, 2653–2657.
- [89] H. Li, C. Guo, T. Zhang, P. Xue, R. Zhao, W. Zhou, W. Li, A. Elzatahry, D. Zhao, D. Chao, *Nano Lett.* **2022**.
- [90] L. Cao, D. Li, F. A. Soto, V. Ponce, B. Zhang, L. Ma, T. Deng, J. M. Seminario, E. Hu, X. Q. Yang, P. B. Balbuena, C. Wang, *Angew. Chem. Int. Ed.* **2021**, *60*, 18845–18851; *Angew. Chem.* **2021**, *133*, 18993–18999.

Manuscript received: November 17, 2022

Revised manuscript received: January 30, 2023

Accepted manuscript online: February 5, 2023

Version of record online: February 23, 2023